Roles of Metal Ion Complexation and Membrane Permeability in the Metal Flux through Lipophilic Membranes. Labile Complexes at Permeation Liquid Membranes

ARTICLE *in* ANALYTICAL CHEMISTRY · SEPTEMBER 2006

Impact Factor: 5.64 · DOI: 10.1021/ac060299p · Source: PubMed

4 AUTHORS, INCLUDING:

Piet W N M van Leeuwen
Institut National des Sciences Appliquées d…
505 PUBLICATIONS **17,562** CITATIONS
SEE PROFILE

Kamil Wojciechowski
Warsaw University of Technology
52 PUBLICATIONS **426** CITATIONS
SEE PROFILE

Anal. Chem. **2006,** *78,* 5693−5703

Roles of Metal Ion Complexation and Membrane Permeability in the Metal Flux through Lipophilic Membranes. Labile Complexes at Permeation Liquid Membranes

Zeshi Zhang,[†] Jacques Buffle,*[,†] Herman P. van Leeuwen,[†,‡] and Kamil Wojciechowski[†]

CABE, Department of Inorganic, Analytical and Applied Chemistry, University of Geneva, Sciences II, 30 quai E. Ansermet, CH-1211 Geneva 4, Switzerland, and Laboratory of Physical Chemistry and Colloid Science, Wageningen University, Dreijenplein 6, NL-6703 HB Wageningen, The Netherlands

The various physicochemical factors that influence the flux of carrier-transported metal ions through permeation liquid membranes (PLM) are studied systematically. Understanding PLM behavior is important (i) to optimize the application of PLM as metal speciation sensors in environmental media and (ii) because PLM may serve as bioanalogical devices that help to elucidate the environmental physicochemical processes occurring at the surface of biological membranes. Diffusion of free and complexed metal ions in solution, as well as diffusion of the metal carrier complex in the membrane, is considered. The respective roles of diffusion layer thickness, ligand concentration, complex stability, carrier concentration, and membrane thickness are studied experimentally in detail and compared with theory, using various labile complexes, namely, Pb(II)−diglycolate, Cu(II)−diglycolate, and Cu(II)−*N*-(2-carboxyphenyl)glycine. Conditions where either membrane diffusion or solution diffusion is rate limiting are clearly discriminated. It is shown in particular, that, by tuning the carrier concentration or membrane thickness, either the free metal ion concentration or the total labile metal species are measured. PLM can thus be used to determine whether models based on the free ion activity in solution (such as BLM or FIAM models) are applicable to metal uptake by microorganisms in a real natural medium.

Metal speciation is being more and more recognized as an essential component of water quality evaluation and is proposed to be incorporated in water quality regulations.[1] As discussed in refs 2 and 3 novel, in situ, real-time dynamic analytical techniques should be developed for that purpose, such as voltammetric sensors,[4] diffusion gradients in thin films,[5] Donnan membrane technique,[6] or permeation liquid membrane (PLM). The principle of the latter was first proposed a few decades ago by Danesi[7] and later developed by a number of researchers (see, for example, ref 8 for review), for industrial selective enrichment of chemicals such as metals, inorganic anions, or organic compounds.[8] The number of reports dealing with trace metal or organic analysis, by PLM or related techniques, is comparatively small[9,10] and even less for metal speciation.[8] Redox speciation of Cr(III/VI)[11] and As(III/V)[12] has been reported. Parthasarathy et al.[13,14] have shown that, under appropriate conditions, PLM is very useful to determine the thermodynamic degree of complexation of metals, in solutions with hydrophilic ligands, either synthetic or natural ones. Analytical applications of PLM to environmental samples have also been reported in refs 15 and 16. Buffle et al.[2] have emphasized that PLM is very appropriate to determine metal complexation in

* Corresponding author: (Fax) +41.22.379.6069; (E-mail) Jacques.Buffle@cabe.unige.ch.

† University of Geneva.

‡ Wageningen University.

(1) Markich, S. J.; Brown, P. L.; Batley, G. E.; Apte, S. C.; Stauber, J. L. *Australas. J. Ecotoxicol.* **2001**, *7*, 109−122.

(2) Buffle, J.; Tercier-Waeber, M.-L. *Trends Anal. Chem.* **2005**, *24*, 172−191.

(3) van Leeuwen, H. P.; Town, R. M.; Buffle, J.; Cleven, R. F. M. J.; Davison, W.; Puy, J.; van Riemsdijk, W. H.; Sigg L. *Environ. Sci. Technol.* **2005**, *39*, 8545−8556.

(4) Buffle, J.; Tercier, M. L. In *In situ monitoring of aquatic systems: Chemical analysis and speciation*; Buffle, J., Horvai, G., Eds.; IUPAC Series on Analytical and Physical Chemistry of Environmental Systems 6; Buffle, J., van Leeuwen, H. P., Series Eds.; Wiley: New York, 2000; Chapter 9.

(5) Davison, W.; Fones, G.; Harper, M.; Teasdale, P.; Zhang, H. In *In situ monitoring of aquatic systems: Chemical analysis and speciation*; Buffle, J., Horvai, G., Eds.; IUPAC Series on Analytical and Physical Chemistry of Environmental Systems 6; Buffle, J., van Leeuwen, H. P., Series Eds.; Wiley: New York, 2000; Chapter 11.

(6) Weng, L.; Temminghoff, E. J. M.; Van Riemsdijk, W. H. *Eur. J. Soil Sci.* **2001**, *52*, 629−637.

(7) Danesi, P. R. *Sep. Sci. Technol.* **1984−85**, *19*, 857−894.

(8) Buffle, J.; Parthasarathy, N.; Djane, N. K.; Matthiasson, L. In *In situ monitoring of aquatic systems: Chemical analysis and speciation*; Buffle, J., Horvai, G., Eds.; IUPAC Series on Analytical and Physical Chemistry of Environmental Systems 6; Buffle, J., van Leeuwen, H. P., Series Eds.; Wiley: New York, 2000; Chapter 10.

(9) Jönsson, J.-A.; Mathiasson, L. *Trends Anal. Chem.* **1992**, *11*, 106.

(10) Papantoni M.,; Djane, N.-K.; Ndungu, K.; Jönsson, J.-A.; Matthiasson, L. *Analyst* **1995**, *120*, 1471.

(11) Djane, Nii-Kotey; Ndung'u, Kuria; Johnsson, Carin; Sartz, Helen; Tornstrom, Tina; Mathiasson, Lennart. *Talanta* **1999**, *48*, 1121−1132.

(12) Li, L. Q.; Yan, P.; Gao, W. Z.; Li, Y. D. *Fresenius' J. Anal. Chem.* **1999**, *363*, 317−319.

(13) Parthasarathy, N.; Buffle, J. *Anal. Chim. Acta* **1994**, *284*, 649−659.

(14) Parthasarathy, N.; Buffle, J.; Gassama, N.; Guenod, F. *Chem. Anal. (Warsaw)* **1999**, *44*, 455−470.

(15) Ndungu, K.; Hurst, M. P.; Bruland, K. W. *Environ. Sci. Technol.* **2005**, *39*, 3166−3175.

(16) Shkinev, V. M.; Fedorova, O. M.; Spivakov, B. Y.; Mattusch, J.; Wennrich, R.; Lohse, M. *Anal. Chim. Acta* **1996**, *327*, 167−174.

10.1021/ac060299p CCC: $33.50
Published on Web 07/07/2006

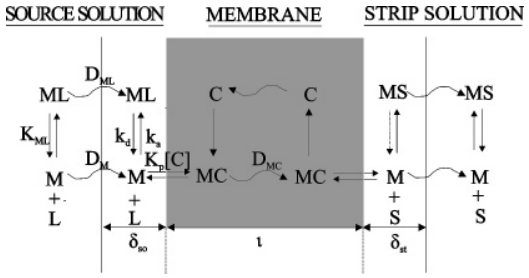

Figure 1. Schematic representation of the transfer of metal ion, M, through a PLM, in the presence of ligand, L, and of ML complex in the test solution.[22] C, carrier; S, complexant of the strip solution; K_{ML}, stability constant of ML; K_p, distribution coefficient of M between the two phases; k_a, k_d, association and dissociation rate constant of ML; D_M, D_{MC}, diffusion coefficients of M in solution and MC in the membrane; δ_{so},δ_{st}, diffusion layer thickness in the source and strip solutions.

complicated environmental systems[8] and can be used as a bioanalogical sensor, i.e., a sensor whose response is controlled by the same environmental processes as those influencing metal uptake by organisms. Various types of PLM devices have been developed, based on (i) batch twin cells[8,17] or flow-through cells[18] combined with flat sheet membranes, (ii) microflow-through cell with integrated voltammetric detector,[19] (iii) hollow fiber membrane,[20] or (iv) emulsion liquid membrane.[21] In many cases,[13,14] it has been shown that, in the presence of ligand, the free metal ion is measured. However, it has also been shown[18] that either free metal ion concentration or the total concentration of labile complexes can be measured, depending on conditions. The main purpose of this paper is to study systematically the factors that influence the flux of metal ion through the PLM, when labile complex-forming ligands are present in solution, to better understand the physicochemical basis of metal speciation measurements by PLM and to optimize the PLM sensor for environmental applications.

In the presence of hydrophilic ligand L, both the free metal ion, M, and its complex, ML, are subject to diffusion in the test (or source) solution, but only free M can be exchanged at the solution/membrane interface (Figure 1). M is then transported by diffusion through the membrane, in the form of the metal−carrier complex, MC, and finally exchanged and accumulated into the receiving (= strip) solution. The major processes and related physicochemical parameters that influence the metal flux through the PLM[8] are depicted in Figure 1. The important parameters are the thickness of the liquid membrane (l), the partition coefficient (K_p) of the metal between the solution and the membrane and its diffusion coefficient (D_{MC}) in the membrane, the carrier concentration in the membrane [C], the diffusion coefficients of the free metal ion, M (D_M), and the metal complex, ML (D_{ML}), in the source solution, the corresponding diffusion layer thickness (δ_{so}) fixed by the hydrodynamic conditions in the source solution, and the degree of lability of ML. The latter is defined by the ratio of the formation rate of ML to the diffusion rate of M toward the membrane.[3] In this paper, only labile complexes will be considered, i.e., complexes that dissociate and reassociate so quickly that diffusion of M and ML is the only rate-controlling step in solution. As will be shown later, the diffusion and complexation parameters related to the receiving (or strip) solution (subscript st) are not relevant in this paper because the conditions are such[8,22] that the corresponding processes are not rate limiting for the accumulation of M in the strip solution.

In the present work, we have tested the effects of the degree of complexation of M, the diffusion layer thickness, the partition coefficient, the membrane thickness, and the carrier concentration on the metal flux, in the framework of a uniform theory, by using the labile complexes of Cu(II) with diglycolate and *N*-(2-carboxyphenyl)glycine, and those of Pb(II) with diglycolate. The roles of l, K_p, and metal−carrier reaction in the presence of a noncomplexing source solution, as well as the role of the strip parameters, are discussed elsewhere.[17,22−24]

THEORY

Stability and Lability of Metal Complexes. In the following, only 1:1 metal complexes will be considered, with association and dissociation rate constants, k_a and k_d, respectively, and the stability constant, $K = k_a/k_d$:

$$\mathrm{M} + \mathrm{L} \underset{k_d}{\overset{k_a}{\rightleftharpoons}} \mathrm{ML} \tag{1}$$

The degree of lability of complexes diffusing toward a consuming interface can be compared through their lability index, L[3]. When the ligand $\mathscr{L}$ is in excess with respect to M and diffusion occurs at planar interface, $\mathscr{L}$ can be expressed by

$$\mathscr{L} = \frac{k_d^{1/2}(1 + \epsilon K[\mathrm{L}])^{1/2}}{\epsilon D_{ML}^{1/2} K[\mathrm{L}]}\delta_{so} \tag{2}$$

where δ_{so} is the diffusion layer thickness, $\epsilon = D_{ML}/D_M$, and [L] is the concentration of free L. [L] is related to the total concentration, $[\mathrm{L}]_t$, by

$$[\mathrm{L}] = \frac{[\mathrm{L}]_t}{(1 + \sum_i \beta_{H,i}[\mathrm{H}]^i)} \tag{3}$$

where the $\beta_{H,i}$'s are the cumulative acid−base stability constants of L ($\beta_{H_i} = K_{H,1}K_{H,2}...K_{H,i}$). Physically, $\mathscr{L}$ represents the ratio between the metal flux when it is fully controlled by the rate of ML dissociation (Figure 1) to the flux entirely controlled by diffusion of M and ML in solution (i.e., assuming very fast dissociation of ML). When $\mathscr{L} \gg 1$, the metal complex is fully labile, whereas for $\mathscr{L} < 1$, the metal complex is nonlabile (flux controlled by dissociation rate). For $\mathscr{L}$ of order of 1, the complex is called semilabile.

(17) Guyon, F.; Parthasarathy, N.; Buffle, J. *Anal. Chem.* **1999**, *71*, 819−826.
(18) Tomaszewski, L.; Buffle, J.; Galceran, J. *Anal. Chem.* **2003**, *75*, 893−900.
(19) Salaun, P.; Berdondini, L.; Bujard, F.; Koudelka-Hep, M.; Buffle, J. *Electroanalysis* **2004**, *16*, 811−820.
(20) Parthasarathy, N.; Pelletier, M.; Buffle, J. *Anal. Chim. Acta* **1997**, *350*, 183−195.
(21) Li, L.-Q.; Zhang, Y.-H.; Gan, W.-E.; Li, Y.-D. *At. Spectrosc.* **2001**, *22*, 290−294.
(22) Salaun, P.; Buffle, J. *Anal. Chem.* **2004**, *76*, 31−39.
(23) Guyon, F.; Parthasarathy, N.; Buffle, J. *Anal. Chem.* **2000**, *72*, 1328−1333.
(24) Wojciechowski, K.; Buffle, J. *Biosens. Bioelectrom.* **2004**, *20*, 1051−1059.

Table 1. Acid−Base Stability Constants of the Tested Ligands[26a]

	diglycolic acid	*N*-(2-carboxyphenyl)glycine
log K_{H1} (M^{-1})	3.94 ± 0.02	4.90 ± 0.01
log K_{H2} (M^{-1})	2.82 ± 0.01	3.33 ± 0.03

[a] I = 0.1 M, T = 25 °C. K_{H1} and K_{H2} are successive stability constants.

Table 2. Stability and Rate Constants of Cu(II) and Pb(II) Complexes with the Tested Ligands

	ref	Pb(II)−diglycolate	Cu(II)−diglycolate	Cu(II)−*N*-(2-carboxyphenyl)glycine
log K_{os} (M^{-1})		1.13	1.13	1.13
log k_{-w} (s^{-1})	28	9.85	9	9
log k_a ($M^{-1}s^{-1}$)		11.0	10.13	10.13
log k_d (s^{-1})		6.6 ± 0.1	6.18 ± 0.02	3.48 ± 0.01
log K (M^{-1})	26	4.4 ± 0.1	3.95 ± 0.2	6.65 ± 0.12

[a] K_{os} and the rate constants (except k_{-w}) were computed as explained in the text. I = 0.1 M, T = 25 °C. The values of the diffusion coefficients of the complexes were taken as equal to those of free metal ions ($D_{ML} = D_M$), with $D_{Pb} = 9.5 \times 10^{-6}$ cm^2 s^{-1} and $D_{Cu} = 7.8 \times 10^{-6}$ cm^2 s^{-1}.[27]

By assuming that the Eigen mechanism holds,[25] i.e., that the limiting step for the formation rate of ML is the dehydration of M, k_a and k_d can be computed by

$$k_a = K_{os}k_{-w} \quad \text{and} \quad k_d = k_a/K \tag{4}$$

where K_{os} is the stability constant of the precursor outer-sphere complex between the hydrated M and L and k_{-w} is the rate constant of water loss from the inner hydration sphere of M. K_{os} is expressed by[25]

$$K_{os} = \frac{4\pi Na^3}{3}\exp\left[-\frac{z_M z_L e^2}{\pi\epsilon_0\epsilon k_B T a}\right]\exp\left[\frac{z_M z_L e^2}{4\pi\epsilon_0\epsilon k_B T(1+\kappa a)}\right] \tag{5}$$

with $\kappa = (2Ne^2I/\epsilon_0\epsilon k_B T)^{1/2}$, N is the Avogadro number (mol^{-1}), a is the distance of closest approach between M and L (m), k_B is the Boltzmann constant (J K^{-1}), e is the charge of an electron (C), ϵ_0 is the vacuum permittivity (8.854×10^{-12} J^{-1} C^{-2} m^{-1}), ϵ is the relative permittivity of water (78.54 at 25 °C), I is the ionic strength (in mol m^{-3}), and z_M, z_L are the number of charges of M and L.

The physicochemical parameters used in this paper are listed in Tables 1 and 2.

The lability index, $\mathcal{L}$, of the three tested metal complexes were computed via eq 2 for the minimum and maximum total concentrations of L used experimentally, by means of the values of Tables 1 and 2. Minimum and maximum values of $\mathcal{L}$, $\mathcal{L}_{min}$, and $\mathcal{L}_{max}$ correspond to maximum and minimum concentrations of L, respectively (eq 2). For Cu and Pb diglycolate complexes, $\mathcal{L}_{min}$ and $\mathcal{L}_{max}$ are independent of pH in the pH range 5−7 and are given in Table 3. For Cu(II)−*N*-(2-carboxyphenyl)glycine, $\mathcal{L}_{min}$ and $\mathcal{L}_{max}$ vary with pH, as shown in Figure 2. Table 3 and Figure 2 show that in all cases, $\mathcal{L}$ values are much larger than 1, indicating that, under the studied conditions, the test complexes are fully labile.

(25) Basolo, F.; Pearson, R. G. *Mechanisms of Inorganic Reactions.* 2nd ed.; Wiley: New York, 1967.

Table 3. Values of $\mathcal{L}_{min}$ and $\mathcal{L}_{max}$ Computed from Eq 2 for the pH Range 5−7[a]

	Pb(II)	Cu(II)
$\mathcal{L}_{max}$	5034 (0.1)	2376 (0.5)
$\mathcal{L}_{min}$	606 (5.0)	770 (4.0)

[a] Total ligand concentrations (in mM) are given in parentheses and correspond to extreme conditions used in this work.

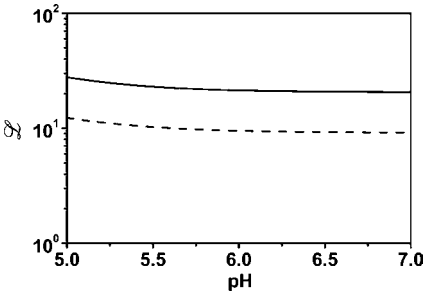

Figure 2. pH dependence of $\mathcal{L}_{min}$ (dashed line, $[L]_t$ = 0.1 mM) and $\mathcal{L}_{max}$ (solid line, $[L]_t$ = 0.01 mM) for Cu(II)−*N*-(2-carboxyphenyl)-glycine.

PLM Metal Flux for Fully Labile Complexes in the Source Solution. The derivation of the theoretical equations for the flux of M in the presence of labile complexes has been described elsewhere.[8,22] It would be out of scope to discuss it here in detail, but it may be useful to recall that the PLM technique uses solvents with very low polarity (in our case, toluene/phenylhexane, with dielectric constant ~2), in which free ions cannot exist. Thus, the carrier (C in Figure 1) must include a lipophilic anion (in our case, anion of fatty acid: laurate or palmitate) and a lipophilic complexant (in our case, the crown ether 22DD = 1,10-didecyl-1,10-diaza-18 crown-6). It has been demonstrated[23] that the complex MC is indeed neutral by including 22DD and 2 mol of laurate/mol of divalent M ion. In addition, it has also been demonstrated[17] that the transport of M does not give rise to charge accumulation, because 2 mol of Na^+ is back transported by the carrier, for each mole of diffusing divalent M. Thus, no significant electrical potential difference is developed across the membrane.

Under such conditions, it has been shown[22] that the metal flux, J, through the membrane is given by eq 6, provided that steady-state conditions exist; i.e., constant concentration gradients are established in the source and membrane phases, and that any process at the membrane/solution interface as well as any chemical reaction inside the solution or membrane phases is fast compared to diffusion.

$$J = \frac{C_{so}^b}{\alpha_{so}}\left(\frac{\delta_{so}}{\bar{D}_{so}\alpha_{so}} + \frac{l}{K_p[C]D_{MC}} + \frac{h_{st}}{2\bar{D}_{st}\alpha_{st}}\right)^{-1} \times \exp\left[-\frac{t}{h_{st}\alpha_{st}}\left(\frac{\delta_{so}}{\bar{D}_{so}\alpha_{so}} + \frac{l}{K_p[C]D_{MC}} + \frac{h_{st}}{2\bar{D}_{st}\alpha_{st}}\right)^{-1}\right] \tag{6}$$

C^b_{so} is the total metal concentration in bulk source, D_{MC} is the diffusion coefficient of the metal−carrier complex, l is the thickness of the membrane, K_p is the partition coefficient of metal between the aqueous phase and the membrane phase, and [C] is the carrier concentration in the membrane. $\bar{D}_{so}$ is the average diffusion coefficient of M and ML, given by[29]

$$\bar{D}_{so} = D_M/\alpha_{so} + D_{ML}(\alpha_{so} - 1)/\alpha_{so} = D_M(1 + \epsilon K[L])/\alpha_{so} \quad (7)$$

with

$$\alpha_{so} = 1 + K[L] \quad (8)$$

α_{st} and $\bar{D}_{st}$ are the equivalent of α_{so} and $\bar{D}_{so}$, for the strip solution, and h_{st} is the depth of the strip channel.

Generally, a very strong ligand is used in the strip solution. *trans*-1,2-Diaminocyclohexane-*N*,*N*,*N*′,*N*′-tetraacetic acid monohydrate (CDTA) was used here. By using the typical parameters of the flow cell system (see Experimental Section), the stability constants of Pb(II)− and Cu(II)−CDTA complexes, and taking $\epsilon \sim 1$, one gets $h_{st}/2\bar{D}_{st}\alpha_{st} = 1.6 \times 10^{-8}$ s cm^{-1} for Cu(II) and 4.2×10^{-10} s cm^{-1} for Pb(II). These values are much smaller than the values of $l/K_p[C]D_{MC}$ for Cu(II) (37.0) or Pb(II) (1.65). The strip solution term can thus be omitted from eq 6. In addition, it is observed that the term in the exponential is extremely small for several hours, so that during that time, the flux is constant and equal to the flux, J^0, at $t = 0$:

$$J^0 = \frac{C^b_{so}}{\alpha_{so}}\left(\frac{\delta_{so}}{\bar{D}_{so}\alpha_{so}} + \frac{l}{K_p[C]D_{MC}}\right)^{-1} = [M]\left(\frac{\delta_{so}}{\bar{D}_{so}\alpha_{so}} + \frac{l}{K_p[C]D_{MC}}\right)^{-1} \quad (9)$$

or

$$P = \frac{J^0}{[M]} = \frac{1}{\frac{\delta_{so}}{\bar{D}_{so}\alpha_{so}} + \frac{l}{K_p[C]D_{MC}}} \quad (10)$$

Equations 9 and 10 enable us to define two useful parameters.

(1) The permeability, P: $P = J^0/[M]$ is a characteristic of the system under the experimental conditions used, independent of metal concentration. The parameter P' will also be used in this paper.

$$P' = \frac{J^0}{C^b_{so}} = \frac{1}{\frac{\delta_{so}}{\bar{D}_{so}} + \frac{l\alpha_{so}}{K_p[C]D_{MC}}} \quad (10')$$

(2) The permeability index, π: π is the ratio of the two terms in the denominator of eq 10. It represents the relative importance of diffusion in solution and in the membrane, for the overall flux.

$$\pi = \frac{\delta_{so}K_p[C]D_{MC}}{\bar{D}_{so}l\alpha_{so}} \quad (11)$$

For $\pi \ll 1$, diffusion in the membrane is the rate-limiting step. Then the first term in the parentheses of eq 9 cancels and J^0 is proportional to free M concentration, irrespective of the degree of complexation in solution.

For $\pi \gg 1$, diffusion in solution is the rate-limiting step. Then the second term in the parentheses of eq 9 cancels and J^0 is proportional to the total concentration of labile M species, C^b_{so}.

Note that this is valid for fully labile complexes only. For inert or semilabile complexes, the expression of π is different. Also note that, in principle, π can be manipulated by adjusting [C], l, or δ_{so} (hydrodynamic conditions), so that in the same solution, one can determine either [M] or C^b_{so} by measuring J^0 under various conditions.[18] It is the purpose of this paper to demonstrate the influence of the various parameters in π, on J^0.

It is useful to combine eqs 9 and 10, with eq 11, to give

$$J^0 = \frac{C^b_{so}\bar{D}_{so}}{\delta_{so}}\left[\frac{\pi}{\pi + 1}\right] \quad (12)$$

and

$$P' = \frac{\bar{D}_{so}}{\delta_{so}}\left[\frac{\pi}{\pi + 1}\right] \quad (13)$$

where $P' = J^0/C^b_{so} = P/\alpha_{so}$. The plot of log P' versus log π (see, for example, Figure 10) tends to linearity for extreme values of π. For $\pi \gg 1$ (in practice $\pi > 10$), log P' tends to the constant value of $\log(\bar{D}_{so}/\delta_{so})$. For $\pi \ll 1$ (in practice $\pi < 0.1$), log $P' = \log(\bar{D}_{so}/\delta_{so}) + \log \pi$, i.e., a straight line with slope = 1. The transition between the two linear regimes occurs around $\pi = 1$. Thus, such plots, which can be obtained by varying any of the parameters determining π (eq 11), clearly show in which regime the system is working.

EXPERIMENTAL SECTION

Reagents and Membrane. The following reagents used for transport experiments were analytical reagents: 2-(*N*-morpholino)-ethanesulfonic acid (MES, Sigma), CDTA (Fluka), sodium hydroxide and lithium hydroxide (Merck), and palmitic acid (PA, Fluka). 1,10-Didecyl-1,10-diaza-18-crown-6 ether (Kryptofix 22DD, Merck), diglycolic acid (Merck), and *N*-(2-carboxyphenyl)-glycine (Aldrich) were pure for synthesis (>98%). The sol-

(26) Martell, A. E.; Smith, R. M. *NIST Critically Selected Stability Constants of Metal Complexes*; v.5.0, U.S. Dept. of Commerce, Technical Administration, 1998.

(27) von Stackelberg, M.; Pilgram, M.; Toome, V. *Z. Elektrochemistry* **1953**, *57*, 342.

(28) Morel, F. M. M.; Hering, J. G. *Principles and applications of aquatic chemistry*; John Whily & Sons Inc.: New York, 1983.

(29) Heyrovsky, J.; Kuta, J. *Principles of Polarography*; Academic Press: New York, 1966.

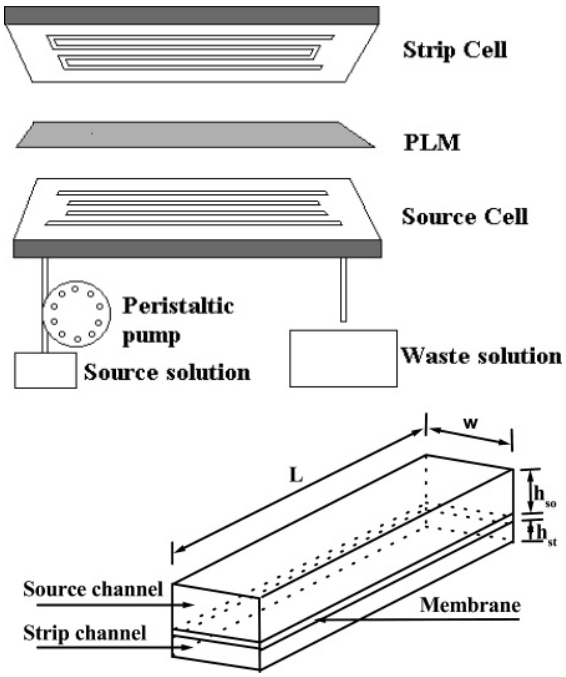

Figure 3. Flow-through cell system and its dimensions. *L*, length of the source channels (12 cm); *W*, width of the channels (1 mm); h_{so}, depth of the source channel (0.6 mm); h_{st}, depth of the strip channel (0.4 mm); effective strip volume, 192 μL.

vents, toluene and phenylhexane, were Fluka analytical grade products. MilliQ water was used for preparing all the aqueous solutions.

The source solution contained the desired concentrations of Cu(II) or Pb(II) (usually 5 μM) in 0.01 M MES (pH 6 was adjusted with LiOH). The strip solution was composed of 0.01 M CDTA (pH 6.20 adjusted with NaOH). The membrane solution was made of 1:1 22DD/PA in 1:1 (v/v) mixture of phenylhexane and toluene. Note that, compared to previous work, palmitate was used instead of laurate in the present study. Indeed, it was observed that, even though the 1:1 mixture 22DD/laurate works as a very good carrier at 0.1 M in organic solvent,[13,14,17,18] its efficiency decreases at lower concentrations and becomes nil at millimolar concentrations. This was attributed to the loss of laurate due to its solubility in water. Systematic studies with laurate, myristate, and palmitate at low concentrations of 1:1 fatty acid/22DD mixtures have shown that the use of palmitate indeed results in excellent Cu(II) and Pb(II) transport, down to ~0.01 M carrier concentration, with flux characteristics stable for days.

Celgard 2500 polypropylene hydrophobic membrane (Celanese Plastic, Charlotte, NC) was used as flat sheet support. Its characteristics are as follows: porosity 0.45; thickness 25 μm; average pore diameter 0.04 μm.

PLM Device and Its Characteristics. A schematic view of the flow-through cell system used in this work and its corresponding characteristics are shown in Figure 3. A peristaltic pump (Gilson, Omnilab) was used to control the source volume flow rate. Standard tubings (Tygon R3607, i.d. = 2.29 mm and 3.175 mm, Biosystems, Omnilab) were used to connect the source solution to the flow-through cell. This cell has been described in detail in ref 18. The source solution flows through four channels in parallel. The metal from the source solution passes through the flat membrane (Figure 3) and accumulates in the stagnant strip channel solution. The strip channel is made of four arms positioned exactly opposite the source channels and connected to each other to form one single channel. The strip solution was collected by a pump at the end of the accumulation period, and the corresponding metal concentration was measured by flame or flameless atomic absorption spectrometry (AAS) using a Pye Unicam SP9 or a Perkin-Elmer 4100 with HGA 700 graphite furnace spectrophotometers. This system enables us to define optimum geometries for the strip and source channels. The strip channel depth, h_{st}, should be sufficiently small to get a short response time and for eqs 9 and 10 to be valid. The depth, h_{so}, width, *W*, and length, *L*, of the source channel (Figure 3) together with the solution flow rate provide a well-defined thickness of the diffusion layer, δ_{so}:[18]

$$\delta_{so} = 0.901 D_{so}^{1/3} d^{1/3} h_{so}^{2/3} L^{1/3} \nu^{-1/3} \qquad (14)$$

where $d = W/2$ = half-width, ν is the volume flow rate, and the numerical coefficient is valid for CGS units.

The major advantages of this cell are the following: a small strip volume yields a high preconcentration factor (defined as $F = C_{st}^{b}/C_{so}^{b}$) in a relatively short time; δ_{so} is well-controlled and tunable by the source flow rate; the total metal concentration in the bulk source solution can be kept constant since the volume of source solution may be very large.

α_{st} was calculated to be $10^{11.2}$ and $10^{12.7}$ for Cu(II)− and Pb(II)−CDTA complexes, respectively, based on the stability constants given in ref 26. Usually, one membrane ($l = 25$ μm) was used, but in some experiments, *l* was varied by stacking several membranes together.

Values of K_p and D_{MC} for Pb(II) and Cu(II) with the system 0.1 M 22DD/0.1 M palmitate were measured as described in ref 17, from extraction and flux experiments performed in the static diffusion cell shown in ref 23. Formation of white microcrystals was observed on the source side of the membrane, at high concentrations (≥50 μM) of Pb(II) and at the end of flux experiments (2−7 h). ATR−IR analysis showed that this solid contained Pb−palmitate. Similar solid formation was observed with Cu(II). Such solids were never observed with the flow-through cell, which is probably due to a combination of two characteristics of flow-through cell experiments: (i) the much lower total metal concentration used (≤5 μM) and (ii) the much smaller contact time between the source solution and the PLM (≤4 s). On the other hand, due to the "static" conditions required for their measurement, D_{MC} and K_p, may contain errors due to formation of colloidal solid, not visible by eye, even though conditions were used to minimize such solid formation. The values of D_{MC} are obtained from the metal flux through the static diffusion cell mentioned above, by plotting $F = C_{st}/C_{so}$ as a function of time. At sufficiently large membrane thicknesses, the $F(t)$ curve shows a time lag at short time, which allows determination of D_{MC}. Because D_{MC} is measured at very short times (few minutes), the possible surface precipitation can be considered as negligible or small during that time. The reproducibility of D_{MC} values was tested by varying the overall membrane thickness, by stacking either three ($l = 75$ μm) or six Celgard membranes ($l = 150$ μm) together. Values of $(3.6 \pm 1.2) \times 10^{-8}$ cm^2/s and

$(4.9 \pm 1.0) \times 10^{-8}$ cm^2/s were obtained for Pb(II) and Cu(II), respectively. These values are close to each other as expected, and the value for Cu(II) is also close to that obtained for Cu(II) with the 0.1 M 22DD + 0.1 M laurate system (5.2×10^{-8} cm^2/s [17]).

Precise determination of the K_p values by liquid−liquid extraction is more difficult, since the contact time between the aqueous and organic solutions is necessarily long. Experiments were performed, as discussed in ref 23, under conditions minimizing artifacts due to colloidal solid formation, as much as possible. Nevertheless the reproducibility of the obtained values of $K_p = [MC]_m/[M]_{so}[C]_m$ (subscript m represents the membrane) was not good. Their ranges are $(1-6) \times 10^5$ and $(1-4) \times 10^4$ M^{-1} for Pb(II) and Cu(II), respectively, at pH 6 and ionic strength of 0.01 M. They should only be considered as orders of magnitude for comparison purposes. To get more precise values of K_p, the PLM data reported in the rest of the paper were fitted with theoretical eqs 10−13, in which K_p is the only adjustable parameter. For all Cu(II) data, a single K_p value was obtained from these fittings. A similar procedure was used for Pb(II). The K_p values obtained in this way were 4.2×10^5 and 1.37×10^4 M^{-1} for Pb(II) and Cu(II), respectively, which are in reasonable agreement with the above orders of magnitude. Considering that the mechanism of transfer of metal at the membrane interface is not simple[24] and not necessarily the same for extraction and PLM experiments, we believe that the K_p values determined by the fitting procedure are the most appropriate for interpretation of PLM data.

Conditions of Metal Transport Experiments. *Flow-Through Cell Preparation and Functioning.* A single membrane (or a set of several membranes stacked together) was impregnated with the membrane solution, as mentioned in ref 18. After rinsing it with water to remove the excess solution, the membrane was clamped tightly and evenly between the source and strip half-cells by 10 screws. The strip solution was injected into the strip channel with a syringe, and then the source solution with given metal concentration was circulated with a constant flow rate. After preconcentration during a given period of time (typically 10−30 min), the strip solution was taken out and Pb(II) or Cu(II) was measured by AAS or flameless AAS. The source channel was then washed by flowing MilliQ water while the strip channel was washed by injecting a new strip solution. Circulation of MilliQ water was performed for up to 25 min, to minimize any carryover effect. Then a new transport experiment was performed with the test source solution and a new strip solution. Usually the initial metal flux and permeability, under one given set of conditions, were computed from four preconcentration experiments performed with different preconcentration times. J^0 was obtained from the slope of the linear plot of the preconcentration factor, F, as a function of time.[18] Typically, such plots do not pass through the origin, since, at the beginning of the experiment, there is ∼1-min time lag (for a single membrane), which corresponds to the transient conditions required to establish the steady-state concentration gradients in the membrane and in solution.

Transport Experiments in the Presence of Complexants. The nature of the complexes used as well as the experimental conditions (pH, ligand concentration) were chosen on the basis of the following criteria: (a) only 1:1 complexes are formed, (b) only fully labile complexes are present (see lability index), and (c) the nature of metals and ligands enables one to span a range of α and π values as wide as possible. For this reason, Cu(II) and Pb(II) complexes of diglycolate and *N*-(2-carboxyphenyl)-glycine were studied in detail. The complexation properties of Cu(II) and Pb(II) with these ligands were determined by titrating a constant ligand concentration with the metal ion and following the Pb^{2+} and Cu^{2+} activities via the potentials of Pb(II) and Cu(II) ion-selective electrodes, with respect to a Ag/AgCl/saturated KCl reference electrode. From the difference between these potentials and those measured in the absence of ligands, α_{so} values were determined (e.g., ref 30) under the experimental conditions used here). We checked that these values compared well with those computed from the stability constants given in the literature.

Transport experiments in the presence of complexants were performed by keeping the total metal (Pb(II) or Cu(II)) concentration constant in the source solution. The total ligand concentration was then varied in such a way that the ligand was always in large excess over metal (0.1−5 mM for Pb−diglycolate and 0.5−4 mM for Cu−diglycolate) and that only the 1:1 metal/ligand complex was formed. For Cu(II)−*N*-(2-carboxyphenyl)glycine, a constant ratio [*N*-(2-carboxyphenyl)glycine]/[Cu(II)] = 20 was used, with the ligand concentration varying from 0.01 to 0.1 mM. The pH of the source solution was always buffered at pH 6.00 with 0.01 M MES (pH adjusted with LiOH). A constant-volume flow rate of 0.02 cm^3/s (corresponding to a linear velocity of 3.33 cm/s) was used for experiments with variable ligand concentrations.

The influence of volume flow rate on the permeability of the membrane in the presence of complexant was determined by varying the flow rate from 0.02 to 0.18 cm^3/s (3.33 to 30.0 cm/s). Metal, 5 μM, with 0.5 mM diglycolate or 0.1 mM *N*-(2-carboxyphenyl)glycine, at pH 6.00 was used for these tests. Other experimental conditions were the same as those discussed above.

The influence of the membrane thickness on the permeability of the membrane was tested in the presence of diglycolate. Several membranes of 25-μm thickness were stacked together and then impregnated with the carrier solution. The membranes stack well together.[23] They were rinsed with water to remove the excess of carrier solution, as explained above for a single membrane. Stacking of one, two, four, and six membranes (corresponding to 25-, 50-, 100-, and 150-μm-thick membranes) were tested under both 0.1 and 0.01 M carrier conditions. The 5 μM concentration of metal with 0.5 mM diglycolate at pH 6.00 was used here, as a test solution.

RESULTS AND DISCUSSION

Metal Permeability in the Presence of Ligands. Typical plots of metal preconcentration versus time, in the absence and presence of ligand, and at two different carrier concentrations, are shown in Figure 4. The experimentally determined preconcentration factor, $F = C^b_{st}/C^b_{so}$, is related to the flux and permeability as follows. At sufficiently short times (scale of hours), the measured flux is equal to the initial steady-state flux, J^0, and is

(30) Buffle, J. *Complexation Reactions in Aquatic Systems*; Ellis Horwood: Chichester, UK, 1988.

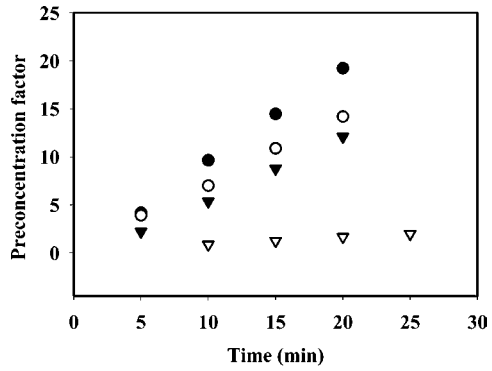

Figure 4. Cu(II) transport under 0.1 and 0.01 M carrier concentrations with and without diglycolate. Source solution: 0.01 M MES, pH 6.00. Strip solution: 0.01 M CDTA, pH 6.20. Volume flow rate: 0.02 cm^3/s ($\equiv$ 3.33 cm/s). ● 0.1 M carrier, without ligand; ○ 0.1 M carrier, with 0.5 mM diglycolic acid; ▼ 0.01 M carrier, without ligand; ▽ 0.01 M carrier, with 0.5 mM diglycolic acid. 5 μM Cu(II) and room temperature in all cases.

related to the increase of metal concentration in the strip solution:

$$J^0 = \frac{V_{st}}{A}\frac{dC^b_{st}}{dt} = h_{st}\frac{dC^b_{st}}{dt} \quad (15)$$

where V_{st} is the volume of strip solution, A is the membrane area in contact with the source solution, and h_{st} is the depth of the strip channel. P' (eq 13) is thus related to F, as follows:

$$P' = \frac{J^0}{C^b_{so}} = h_{st}\frac{dC^b_{st}}{C^b_{so}dt} = h_{st}\frac{dF}{dt} \quad (16)$$

Figure 4 shows that, under the experimental conditions used, the preconcentration factor, F, increases linearly with time, i.e., P' and J^0 are constant. This indeed corresponds to the conditions of the initial flux, which prevails under steady-state conditions (eqs 9, 10). This result is also in agreement with experimental data reported in the literature.[18]

Figure 4 illustrates a few important features of the PLM. For a given accumulation time, the value of F in the absence of diglycolate is much smaller for 0.01 M carrier than for 0.1 M carrier. This suggests that P' is at least partially controlled by the transport through the membrane (eq 10′), which depends on the metal distribution factor, K_p[C], between the membrane and solution phases. Another observation is that, for a given accumulation time and carrier concentration, F is smaller in the presence of diglycolate than in its absence, demonstrating that metal complexation reduces the amount of metal taken up by the membrane. For labile complexes, J^0 and P' are inversely proportional to the degree of complexation, α_{so}, when diffusion in the membrane is the rate-limiting step for transport (eqs 9, 10′). In such a case, α_{so} can be obtained, for a given time, by the ratio of the values of P' with and without ligand. However, when these ratios are computed for [C] = 0.1 M and [C] = 0.01 M for the data of Figure 4, values of 0.69 and 0.14 are obtained, respectively; i.e., a decrease by a factor of 5 instead of 10 is observed. Since the tested complexes are fully labile (Figure 2, Table 3), the fact that P' does not vary with [C] and α_{so} in a linearly proportional manner suggests that diffusion in both the membrane and the solution are limiting steps (eqs 9, 10′); i.e., π is neither $\gg$1 nor $\ll$1. This behavior is quantitatively studied and discussed below.

Changes in P and π with Ligand Concentration. When the ligand concentration increases, the degree of complexation, α_{so} increases, and accordingly, the value of π decreases (eq 11). It is then expected (see eq 13) that, when the value of π in the absence of ligand is not much larger than 1, the metal flux, J^0 (and consequently P') will decrease, possibly passing from source diffusion limitation to membrane diffusion limitation. Figure 5 shows such experiments. Note that each panel a-2 to c-2 of Figure 5 represents the same data as the corresponding panels a-1 to c-1. Only the ligand concentrations (panels 1) have been transformed into π values (panels 2) through eqs 8 and 11. Experiments were carried out at 0.1 M carrier concentration, because under this condition, the permeability in the absence of ligand is fully controlled by diffusion in the source solution, for both Cu(II) and Pb(II). This is shown in Figure 5a-2, b-2, and c-2. Indeed, in all cases, the highest π values (which always correspond to $[L]_t = 0$ and $\alpha_{so} = 1$; eqs 8, 11), are large enough for P' to attain its maximum value (eq 13). Diffusion in solution is then the only rate-limiting factor. Figure 5a-1, b-1, and c-1 also show that P' decreases monotonically with $[L]_t$, but not to the same extent for the three metal−ligand systems. The decrease is very weak for Pb(II)−diglycolate, intermediate for Cu(II)−diglycolate, and very strong for Cu(II)−*N*-(2-carboxyphenyl)glycine. This difference in behavior results from the values of both K_p and α_{so} in each case:

For Pb(II), the K_p value is very large (4.2×10^5), which reflects a strong uptake capability of the membrane. As a consequence, one always gets $\pi > 2$ (Figure 5a-2), even for the largest value of α_{so} (or ligand concentration), over the studied concentration range ($6 < \alpha_{so} < 282$). Thus, P' remains close to its maximum value, irrespective of α_{so} values, as expected from eq 13. Physically, these results can be understood by considering that the uptake by the membrane is so large that, for any value of $[L]_t$, the free M concentration at the membrane surface is nil. Since ML is fully labile (complete equilibrium in the diffusion layer), the surface concentration of ML is also nil, and the overall flux is controlled by the sum of the maximum concentration gradients of both M and ML. Thus, J^0 and P' only depend on C^b_{so}, through $\bar{D}_{so}$.

The Cu(II)-*N*-(2-carboxyphenyl)glycine system is the opposite case. The K_p value (1.37×10^4) is such that π is significantly larger than 1 in the absence of ligand, but not in the presence of the strong ligand *N*-(2-carboxyphenyl)glycine (Figure 5c-2). In the presence of ligand, one always gets $\pi \ll 1$, due to the large values of α_{so} ($86 < \alpha_{so} < 426$ in the tested range of $[L]_t$). Under such conditions, P' is fully controlled by diffusion in the membrane; i.e, the metal flux is much smaller than what it would be if it were controlled by diffusion in solution. Consequently, the gradients in the source solution are insignificant, and the free M concentration at the membrane surface is essentially equal to that in the bulk source solution, [M]. J^0 is then proportional to [M] and not to C^b_{so}. Under such conditions, log P' is proportional to log π, with a slope of 1.0, as theoretically expected (eq 13).

The Cu(II)−diglycolate system (Figure 5b) is an intermediate case. The values of α_{so} are not very large and π only decreases

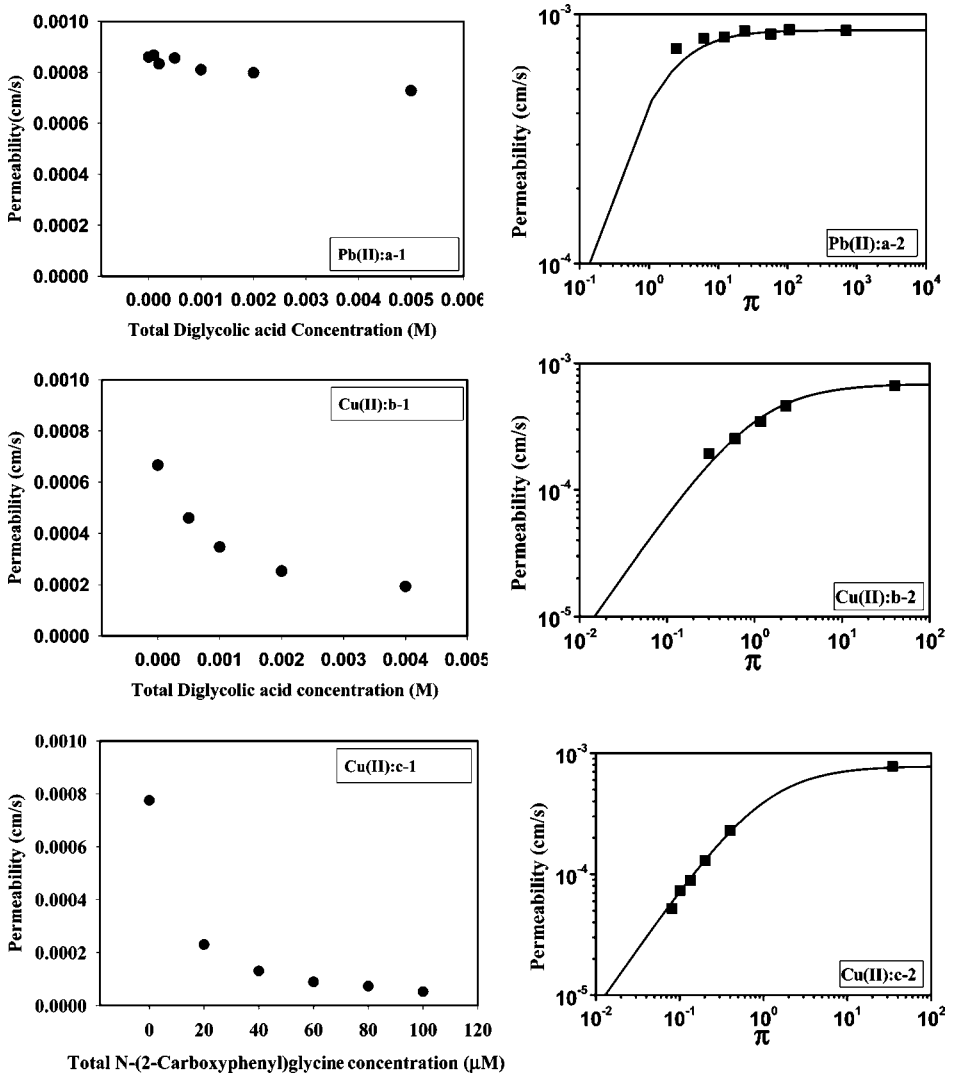

Figure 5. Effect of ligand concentration on the permeabilites, P', of Cu(II) and Pb(II). Source solution: 0.01 M MES, pH 6.00. Carrier: 1/1 mixture of 0.1 M 22DD/0.1 M PA. Strip solution: 0.01 M CDTA, pH 6.20. Volume flow rate: 0.02 cm^3/s (= 3.33 cm/s). 5 μMPb(II) and Cu(II) in the presence of diglycolate (a, b); [*N*-(2-carboxyphenyl)glycine]$_{total}$/[Cu(II)]$_{total}$ = 20 (Figure 5c). Solid lines are theoretical predictions from eq 13). (a-1), (b-1) and (c-1) give the raw data P' vs [L]$_t$, while (a-2), (b-2), and (c-2) give log P' vs log π, where π depends on [L]$_t$ through α_{so} (eq 11).

from 2.12 to 0.28 when the diglycolate concentration varies from 0.5 to 4 mM. These values correspond to fluxes controlled by both diffusion in source solution and diffusion in the membrane, even though the membrane control becomes more and more important when π decreases.

The full lines in Figure 5a-2, b-2, and c-2 are theoretical predictions based on eq 13 for P' and eq 11 for π. In these equations, $\bar{D}_{so}$ was taken as $\bar{D}_{so} = D_M$, which is acceptable, since all ligands are small. The value of δ_{so} was determined experimentally by using eq 9, in the absence of ligands. Then

$$\delta_{so} = D_M\left[\frac{C_{so}^b}{J^0} - \frac{l}{K_p[C]D_{MC}}\right] \qquad (17)$$

Values of 103 μm for Cu(II) and 110 μm for Pb(II) were obtained for the flow rate used, which agree with values obtained from eq 14. Figure 5a-2, b-2, and c-2 demonstrate a good fit between experimental data and theoretical curves.

Impact of the Source Solution Flow Rate (or Diffusion Layer Thickness) on the Permeability, P', at Different π Values. The value of δ_{so} is important since it influences both the lability of the complexes and the metal permeability of the membrane. The theoretical relation between δ_{so} and the flow rate of the source solution, for the flow-through cell used here, has been derived by Tomaszewski et al.,[18] and it has been shown that a well-defined diffusion layer thickness can be obtained by controlling the volume flow rate. Since the complexes used here are fully labile (Figure 2, Table 3), eqs 10′ and 11 predict that P' should depend on δ_{so} for $\pi \gg 1$, while P' should be independent of δ_{so} for $\pi \ll 1$. These predictions were checked by varying the volume flow rate at constant Pb(II)−diglycolate and Cu(II)−*N*-(2-carboxyphenyl)glycine concentrations as shown in Figure 6.

Due to the large K_p value for Pb(II), one gets $\pi > 10$ for the Pb(II)−diglycolate system at all flow rates. Diffusion in the source solution is thus the rate-limiting step in all cases, and P' is then

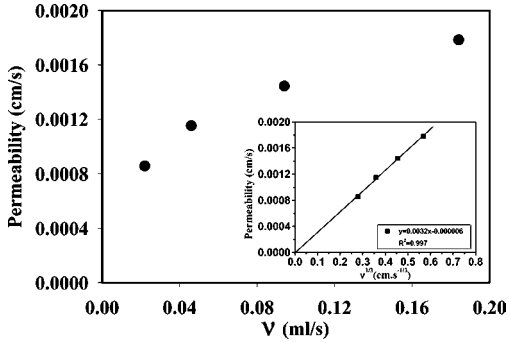

Figure 6. Effect of the volume flow rate, ν, on the permeability, P', of Pb(II) in the presence of diglycolate. Source solution: 0.01 M MES, pH 6.00. Carrier: 1/1 mixture of 0.1 M 22DD/0.1 M PA. Strip solution: 0.01 M CDTA, pH 6.20; 5 μM Pb(II) with 0.5 mM diglycolate. Inset: P' vs $\nu^{1/3}$.

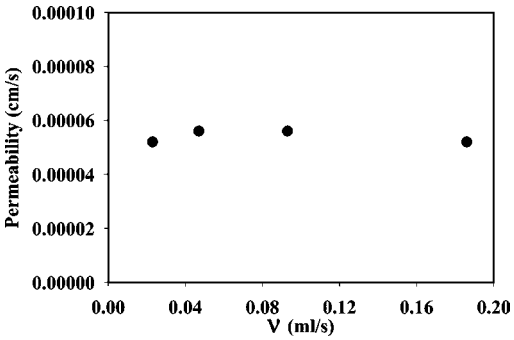

Figure 7. Effect of the volume flow rate, ν, on the permeability, P', of Cu(II), in the presence of *N*-(2-carboxyphenyl)glycine. Source solution: 0.01 M MES, pH 6.00. Carrier: 1/1mixture of 0.1 M 22DD/0.1 M PA. Strip solution: 0.01 M CDTA, pH 6.20; 5 μM Cu(II) with 0.1 mM *N*-(2-carboxyphenyl)glycine; room temperature.

predicted to be inversely proportional to δ_{so} (eq 10′), since $\pi/(\pi + 1) \sim 1$. An increase in the volume flow rate, ν, decreases δ_{so} (eq 14 [18]) and should thus enhance P' and the Pb(II) flux. Figure 6 shows that such a behavior is indeed observed. By plotting P' versus $\nu^{1/3}$, a good straight line is obtained (inset of Figure 6), as expected from eq 14.

Conversely, the π values for the Cu(II)−*N*-(2-carboxyphenyl)-glycine system (5 μM Cu(II), 0.1 mM ligand) are much smaller than 1 at all ν values (see Figure 5c-2). So P' is independent of δ_{so} (or ν; Figure 7) as predicted theoretically by eq 10′. This result also indicates that, under such conditions, the equilibria in solution are not perturbed by the uptake of M at the solution/membrane interface and concentrations of all species are always the same as in the bulk.

Impact of Membrane Thickness and Carrier Concentration on Metal Permeability. By increasing the membrane thickness, l, π decreases (eq 11), which reflects the fact that diffusion through the membrane becomes more demanding. The role of this process, as rate-limiting step, thus increases. The same result should be obtained by decreasing the carrier concentration, [C]. Figure 8 shows that, for Pb(II), either in the absence or the presence of 0.5 mM diglycolate, P' is independent of l. This is coherent with the finding that, for all l values, experimental values of π were larger than 5; i.e., $P' = D_M/\delta_{so}$ (eq 13). Thus, P' is never controlled by membrane diffusion under the current experimental conditions.

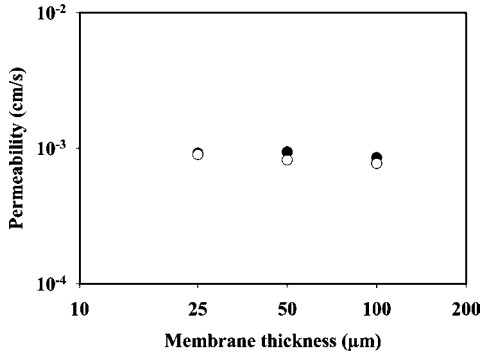

Figure 8. Pb(II) permeability, P', as a function of membrane thickness and carrier concentration. Source solution: 0.01 M MES, pH 6.00. Strip solution: 0.01 M CDTA, pH 6.20. Carrier: 1/1 mixture of 0.1 M 22DD/0.1 M PA. Volume flow rate: 0.02 cm^3/s (≡ 3.33 cm/s). 5 μM Pb(II). Membrane thickness: 25, 50, and 100 μm. Room temperature. ● 0.1 M carrier, without ligand; ○ 0.1 M carrier, with 0.5 mM diglycolic acid.

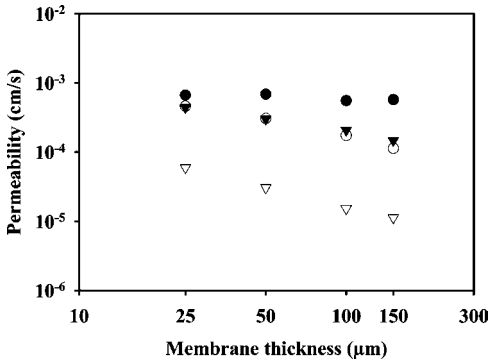

Figure 9. Cu(II) permeability, P', as a function of membrane thickness, and complexant and carrier concentrations. Source solution: 0.01 M MES, pH 6.00. Strip solution: 0.01 M CDTA, pH 6.20. Carrier: 1/1 mixture of 0.1 M 22DD/0.1 M PA (circles) or 0.01 M 22DD/0.01 M PA (triangles). Volume flow rate: 0.02 cm^3/s (≡ 3.33 cm/s). 5 μM Cu(II). Membrane thickness: 25, 50, 100, and 150 μm. Room temperature. ● 0.1 M carrier, without ligand; ○ 0.1 M carrier, with 0.5 mM diglycolic acid; ▼ 0.01 M carrier, without ligand; ▽ 0.01 M carrier, with 0.5 mM diglycolic acid.

Cu(II) shows a completely different behavior (Figure 9). In the absence of ligand, P' passes from a regime controlled by diffusion in solution (P' independent of l) at 0.1 M carrier, C, to a regime controlled by diffusion in the membrane at 0.01 M carrier. Indeed, by decreasing [C], π decreases accordingly, and becomes smaller than 1. When diffusion in the membrane is the only rate-limiting step, eq 13 becomes $P' = D_M\pi/\delta_{so} \sim l^{-1}$. In the presence of diglycolate, with both 0.1 and 0.01 M carrier, the decrease of π is sufficient (as already seen in Figure 5b) to change the rate-controlling step from diffusion in solution to diffusion in the membrane. The corresponding curves in Figure 9 confirm this prediction since straight lines are obtained for log P' versus log l with slopes of −0.78 for 0.1 M carrier and −0.94 for 0.01 M carrier, i.e., close to −1.

Nature of K_p. It seems useful to devote some remarks to the nature of the distribution parameter, K_p. The dependences of π and P' on the various parameters of the systems are generally well predicted by the theory explained in this paper (see above) and the general equation $P' = f(\pi)$ (eq 13). Overall correspondence between experimental data and theory can be

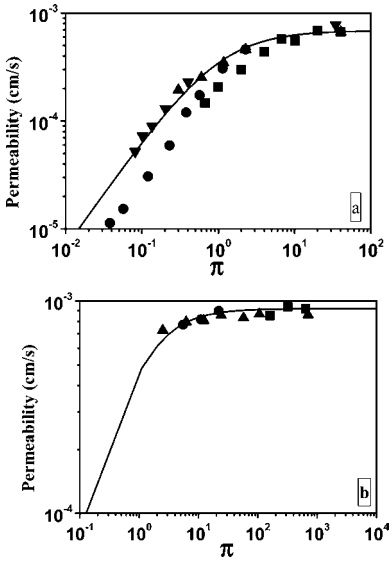

Figure 10. Relation of Cu(II) (a) and Pb(II) (b) permeability, P', with π by varying l, [C], andα_{so}. Conditions of (a): ▲ see Figure 5b, ▼ see Figure 5c, ■ see Figure 9 without ligand, and ● see Figure 9 with ligand. Conditions of (b): ▲ see Figure 5a, ■ see Figure 8 (no ligand), and ● see Figure 8 (0.5 mM ligand).

evaluated from Figure 10, where all the data of Figures 5, 8, and 9 are plotted again as $\log P' = f(\log \pi)$. It can be seen that, for Pb, all data fall on the same curve. For Cu(II), all the data also follow theoretical predictions. However, the curve generated by the data of Figures 8 and 9 is slightly shifted along the π axis compared to the curve based on Figure 5. These different data were obtained from different sets of experiments, and the shift between the two sets would correspond to a difference of a factor of ~2 in the K_p values for the two cases. This suggests that K_p might not be a perfectly well-defined thermodynamic parameter, as is also suggested by other results[24] that point at complicated interfacial processes. Thus, for the carrier system used here, K_p might have a partly operational nature, which may depend somewhat on experimental conditions. Consequently, for precise and reproducible speciation measurements, the calibration must be performed for each set of experiments, with the same experimental system and conditions. A study of the rigorous nature of K_p is in progress.

CONCLUSIONS

The present work shows that the factors of the test medium (δ_{so},α_{so}, $\bar{D}_{so}$) which may affect the metal flux through PLM are quantitatively understood. It is interesting to note that they play the same role in the metal uptake by organisms as in the metal flux through PLM. In fact, provided planar diffusion is valid in both cases, the permeability eqs 11 and 13, developed for PLM, are equally applicable to biouptake. One simply has to replace the PLM membrane rate constant ($k_{PLM} = K_p[C]D_{MC}/l$ in eq 11 by a biological internalization rate constant, k_{int},[2,31] while the rate constant for diffusion in solution, $k_{so} = \bar{D}_{so}\alpha_{so}/\delta_{so}$ remains unchanged. Thus, permeability versus π curves, with shapes similar to those of Figure 5 or 10 are expected for both PLM and organisms. This has interesting implications:

First, it is possible to predict that when the medium becomes more complexing (α_{so} increases) or when convection increases (δ_{so} decreases), the π value for a given organism will decrease, as for PLM. Thus, there is an increased probability that the permeability will only depend on free M concentration (or activity), i.e., that uptake models such as the free ion activity model (FIAM) or the biotic ligand model (BLM)[31] are valid. On the other hand, the chance that metal uptake will depend on the total concentration of labile metal species will increase with decreasing α_{so} values and in poorly mixed systems.

Above all, this work demonstrates that PLM can be used to determine whether biouptake is controlled by free metal ion or by total labile species. Indeed, the PLM flux (permeability) can be tuned at the same value as that of metal uptake by the test organism, by choosing the right value of π, $\pi_{organism}$, via the appropriate adjustment of [C], l, or δ_{so} parameters. Then by measuring and plotting $\log P' = f(\log \pi)$, for π values around $\pi_{organism}$, it is possible to determine whether diffusion in solution (P' independent of π) or transport through the membrane (P' proportional to π) is the rate-limiting step. This conclusion will be valid for both PLM and organism, provided the range of P' used is the same for both.

For experimental reasons, this capability of linking speciation to bioavailability is unique for PLM compared to other dynamic speciation sensors. Thanks to its additional potential capability for in situ measurements in waters, this type of sensor might thus become a major tool in bioenvironmental monitoring.

ACKNOWLEDGMENT

Michel Martin is gratefully acknowledged for performing ICPMS analyses. This work was supported by the Swiss National Foundation (project 20-61871.00). Support was also supplied by the ECODIS project funded by the European Commission 6th framework program, subpriority 6.3 "Global change and ecosystems", under contract 518043.

GLOSSARY

[C]	carrier concentration in the membrane
C^b_{so}	total metal concentration in bulk source solution
C^b_{st}	total metal concentration in bulk strip solutions
$d = W/2$	half-width of the PLM cell channel
D_{MC}	diffusion coefficient of metal−carrier complex in the membrane
D_M	diffusion coefficient of the free metal ion, M, in the source solution
D_{ML}	diffusion coefficient of the metal complex, ML, in the source solution
$\bar{D}_{so}$	average diffusion coefficient of M and ML in the source solution
$\bar{D}_{st}$	average diffusion coefficient of M and MS in the strip solution
F	preconcentration factor
h_{so}	depth of the source channel
h_{st}	depth of the strip channel
I	ionic strengh

(31) Wilkinson, K.; Buffle, J. In *Physico-chemical kinetics and transport at chemical biological interphases*; van Leeuwen, H. P., Köster, W., Eds.; IUPAC Series on Analytical and Physical Chemistry of Environmental Systems; Buffle, J., van Leeuwen, H. P., Series Eds.; Wiley: New York, 2005: Chapter 10.

J	metal flux
J^0	metal flux, at $t = 0$
K	stability constant of the complex ML
$K_{H,i}$	successive ith acid−base stability constant of L
k_a	association rate constant of ML
k_d	dissociation rate constant of ML
K_p	partition coefficient of the metal between the solution and the membrane
l	membrane thickness
[L]	concentration of free ligand, L
$[L]_t$	total ligand concentration
L	length of the source channel
$\mathscr{L}$	lability index
M	metal ion
ML	metal complex in the source phase
MC	metal−carrier complex in the membrane
MS	metal complex in the strip phase
P	permeability
α_{so}	degree of M complexation in the source solution
α_{st}	degree of M complexation in the strip solution
δ_{so}	diffusion layer thickness in the source solution
ν	volume flow rate
π	permeability index

Received for review February 17, 2006. Accepted June 1, 2006.

AC060299P